Optimal design and characteristics analysis of a polymer electro-optic switch with seven vertical-turning serial-coupled microrings*

LUO Qian-qian (罗倩倩), **ZHENG Chuan-tao** (郑传涛)**, **SUN Chang-lun** (孙长轮), **and ZHANG Da-ming** (张大明)

State Key Laboratory on Integrated Optoelectronics, College of Electronic Science and Engineering, Jilin University, Changchun 130012, China

(Received 15 July 2013)

©Tianjin University of Technology and Springer-Verlag Berlin Heidelberg 2013

A novel 1×2 polymer electro-optic (EO) switch based on seven vertical-turning serial-coupled microrings is proposed for dropping crosstalk and obtaining flat boxlike spectrum. The device structure, theory and formulation are presented, and the microring resonance order and coupling gaps are optimized. The switching voltage of the device for obtaining crosstalk lower than −30 dB under through state is decided to be about 1.86 V. Under the operation voltages of 0 V (drop state) and 1.86 V (through state), the switching performance is characterized, and the output spectrum is analyzed. The calculation results show that the crosstalk at through state and that at drop state are −30.2 dB and −53.2 dB, respectively, while the insertion losses are 0.86 dB and 3.18 dB, respectively. Owning to the seven serial-coupled microrings resonance structure, the proposed switch reveals the favorable boxlike spectrum compared with the simple device with only one microring, and thus the crosstalk under drop state is improved from −26.8 dB to −53.2 dB. Due to the low crosstalk, this device can be used in optical networks-on-chip for signal switching and routing.

Document code: A **Article ID:** 1673-1905(2013)06-0425-5

DOI 10.1007/s11801-013-3128-x

Electro-optic (EO) switches[1-6] play a crucial role in the optical communication systems. Poled polymers[7-10] are widely used in the fabrication of optical switches and modulators. In 2009, a polymer EO switch composed of a single microring coupled with two parallel channel waveguides was reported by our group[11]. In this paper, we propose a novel polymer EO switching configuration by using seven vertical-turning serial-coupled microrings, which is an improvement to the structure reported in Ref.[11].

The structure model of the microring resonator (MRR) EO switch is shown in Fig.1(a), which consists of a horizontal channel, a vertical channel and seven vertical-turning serial-coupled microrings. The cross section of MRR waveguide is shown in Fig.1(b). The electrodes are only deposited on microrings, so the EO effect only occurs in the waveguide cores of microrings. The waveguide layers are upper electrode, upper buffer layer, core, under buffer layer and lower electrode. By applying different operation voltages on the microrings, the switching functions can be realized between the horizontal channel and the vertical channel. The device length and width are both $L_1+L_2+L_3$. During design, we select L_1=100 μm, L_3=100+w_c/2, and L_2=3(2R+ w_r)+R+w_r/2+3h_{RR}+h_{CR}+w_c/2, where h_{RR} is the coupling gap between two adjacent microrings, h_{CR} is that between the channel waveguide and MRR waveguide, and w_r and w_c are core widths of the MRR waveguide and channel waveguide, respectively.

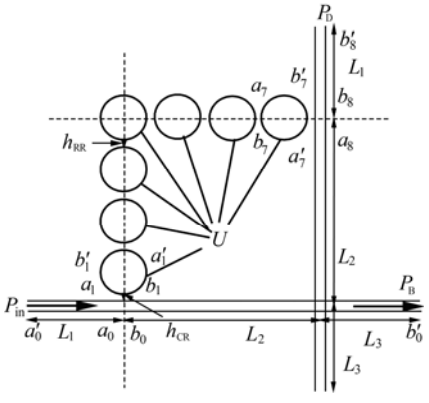

(a)

* This work has been supported by the National Natural Science Foundation of China (Nos.61107021, 61177027 and 61077041), the Ministry of Education of China (Nos.20110061120052 and 20120061130008), the China Postdoctoral Science Foundation Funded Project (Nos.20110491299 and 2012T50297), the Science and Technology Department of Jilin Province of China (No.20130522161JH), and the Special Funds of Basic Science and Technology of Jilin University (Nos.201103076 and 200905005).

** E-mail: zhengchuantao@jlu.edu.cn

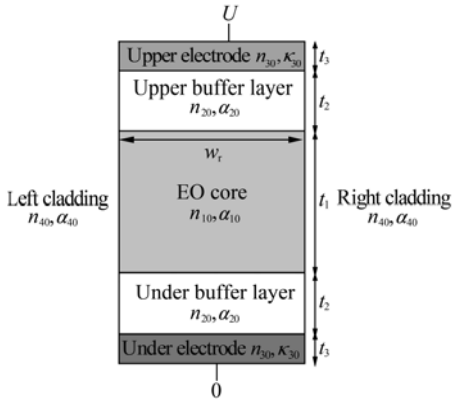

(b)

Fig.1 (a) Structure model of the MRR EO switch based on seven vertical-turning serial-coupled microrings; (b) Cross-section of the MRR waveguide

Under 1550 nm, the related material parameters are taken as follows. The refractive index of the EO polymer material (AJL8/APC) is n_{10} = 1.59, its bulk amplitude attenuation coefficient is α_{10}= 0.25 dB/cm, and its EO coefficient is γ_{33}= 68 pm/V[12]. The refractive index of the upper/under buffer layer material [P(PFS-GMA)] is n_{20} = 1.461, and its bulk amplitude attenuation coefficient is α_{20}= 0.25 dB/cm[13]. The electrode is made of aurum, its refractive index is n_{30} = 0.19, and its bulk extinction coefficient is κ_{30}= 6.1[14]. Air is adopted as the left/right cladding layer, i.e., n_{40} = 1.0 and α_{40}= 0.

The thickness of upper/under buffer layer is taken as t_2=2.5 μm, and the thickness of electrode is taken as t_3=0.2 μm. For assuring single-mode propagation in microring rectangular waveguide, its width and thickness are both taken as w_r=t_1=1.7 μm. We take the ring bending radius as R=19.49 μm, and the calculated mode effective refractive index is about 1.5189 under the case of applying no voltage. We take the core thickness of the channel equal to that of the microring as t_1=1.7 μm, and select the width of the channel as w_c=1.85 μm, and in this case, the channel and microring possess the identical mode effective refractive index. Under the parameters above, the mode loss in MRR waveguide is almost equal to that of the channel waveguide, which is α_R=α_C= 0.256 dB/cm.

For the seven vertical-turning serial-coupled microrings, define κ_{RR} and t_{RR} as the amplitude coupling ratio and amplitude transmission ratio between two adjacent microrings, respectively. Then the relation between the amplitudes a_1, b_1 and a_7', b_7' can be expressed by

$$\begin{bmatrix} a_7' \\ b_7' \end{bmatrix} = \boldsymbol{P}_R \boldsymbol{M} \boldsymbol{P}_R \begin{bmatrix} a_1 \\ b_1 \end{bmatrix} = \boldsymbol{M}_t \begin{bmatrix} a_1 \\ b_1 \end{bmatrix}, \tag{1}$$

where

$$\boldsymbol{P}_R = \begin{bmatrix} 0 & \exp(-j\phi_R) \\ \exp(j\phi_R) & 0 \end{bmatrix} \left(\frac{1}{j\kappa_{RR}} \right)^2 \times \begin{bmatrix} -\exp(j\phi_R) & t_{RR}\exp(-j\phi_R) \\ -t_{RR}\exp(j\phi_R) & \exp(-j\phi_R) \end{bmatrix}^2, \tag{2}$$

$$\boldsymbol{M} = \frac{1}{j\kappa_{RR}} \begin{bmatrix} t_{RR} & -1 \\ 1 & -t_{RR} \end{bmatrix} \begin{bmatrix} 0 & \exp(-j\phi_1) \\ \exp(j\phi_2) & 0 \end{bmatrix} \times \frac{1}{j\kappa_{RR}} \begin{bmatrix} t_{RR} & -1 \\ 1 & -t_{RR} \end{bmatrix}, \tag{3}$$

where $\phi_R = \pi R(\beta_R - j\alpha_R)$, $\phi_1 = \frac{3}{2}\pi R(\beta_R - j\alpha_R)$ and $\phi_2 = \frac{1}{2}\pi R(\beta_R - j\alpha_R)$.

According to EO modulation theory, we can obtain the variation of refractive index Δn_{10} of the EO core material resulting from the operation voltage U as

$$\Delta n_{10}(U) = \frac{1}{2} n_{10}^3 \gamma_{33} E_1 = \frac{n_{10}^3 n_{20}^2 \gamma_{33} U}{2(2n_{10}^2 t_2 + n_{20}^2 t_1)}, \tag{4}$$

where U can be equal to zero or not. The refractive index of the EO core material n_{10} will be changed to $n_{10}+\Delta n_{10}$. Then the mode propagation constant in each microring can be regarded as a function of U, denoted by $\beta_R(U)$. Since ϕ_1, ϕ_2, ϕ_R, κ_{RR} and t_{RR} are all related to mode propagation constant, $\boldsymbol{M}_t$ will be a function of U, that is $\boldsymbol{M}_t$=$\boldsymbol{M}_t(U)$.

The relation between a_0, b_0 and a_1, b_1 is

$$\begin{bmatrix} a_1 \\ b_1 \end{bmatrix} = \frac{1}{j\kappa_{CR}} \begin{bmatrix} t_{CR} & -1 \\ 1 & -t_{CR} \end{bmatrix} \begin{bmatrix} a_0 \\ b_0 \end{bmatrix}, \tag{5}$$

and that between a_7', b_7' and a_8, b_8 is

$$\begin{bmatrix} a_8 \\ b_8 \end{bmatrix} = \frac{1}{j\kappa_{CR}} \begin{bmatrix} t_{CR} & -1 \\ 1 & -t_{CR} \end{bmatrix} \begin{bmatrix} a_7' \\ b_7' \end{bmatrix}, \tag{6}$$

where κ_{CR} and t_{CR} are the amplitude coupling ratio and amplitude transmission ratio between MRR waveguide and channel waveguide, respectively. So the total transfer matrix of the switch can be written as

$$\begin{bmatrix} a_8 \\ b_8 \end{bmatrix} = \frac{1}{j\kappa_{CR}} \begin{bmatrix} t_{CR} & -1 \\ 1 & -t_{CR} \end{bmatrix} \boldsymbol{M}_t \frac{1}{j\kappa_{CR}} \begin{bmatrix} t_{CR} & -1 \\ 1 & -t_{CR} \end{bmatrix} = \boldsymbol{P}_t \begin{bmatrix} a_0 \\ b_0 \end{bmatrix}, \tag{7}$$

where $\boldsymbol{P}_t = \frac{1}{j\kappa_{CR}} \begin{bmatrix} t_{CR} & -1 \\ 1 & -t_{CR} \end{bmatrix} \boldsymbol{M}_t \frac{1}{j\kappa_{CR}} \begin{bmatrix} t_{CR} & -1 \\ 1 & -t_{CR} \end{bmatrix}$ is a 2×2 matrix, and its invert matrix is defined as $\boldsymbol{P}_t^{-1}$. Eq.(7) can be further written as

$$\begin{bmatrix} a_0 \\ b_0 \end{bmatrix} = \boldsymbol{P}_t^{-1} \begin{bmatrix} a_8 \\ b_8 \end{bmatrix}. \tag{8}$$

Considering that $a_8 = 0$, $a_0 = [\boldsymbol{P}_t^{-1}(1,2)]^{-1} b_8$ and $b_0 = \boldsymbol{P}_t^{-1}(2,2) b_8$, we obtain from Eq.(8) that

$$\frac{b_8'}{a_0} = [\boldsymbol{P}_t^{-1}(1,2)]^{-1}, \tag{9}$$

$$\frac{b_0}{a_0}=\frac{\boldsymbol{P}_{\mathrm{t}}^{-1}(2,2)}{\boldsymbol{P}_{\mathrm{t}}^{-1}(1,2)}. \tag{10}$$

Combing the following relations of $a_0=a_0^{'}\exp(-\mathrm{j}\psi_1)$, $b_0^{'}=b_0\exp\left[-\mathrm{j}(\psi_1+\psi_2)\right]$ and $b_8^{'}=b_8\exp(-\mathrm{j}\psi_1)$, the output light amplitudes from the drop port and through port can be finally expressed as

$$\frac{b_8^{'}}{a_0^{'}}=\frac{b_8\exp(-\mathrm{j}\psi_1)}{a_0\exp(\mathrm{j}\psi_1)}=[\boldsymbol{P}_{\mathrm{t}}^{-1}(1,2)]^{-1}\exp(-\mathrm{j}2\psi_1), \tag{11}$$

$$\frac{b_0^{'}}{a_0^{'}}=\frac{b_0\exp\left[-\mathrm{j}(\psi_1+\psi_2)\right]}{a_0\exp(\mathrm{j}\psi_1)}=\frac{\boldsymbol{P}_{\mathrm{t}}^{-1}(2,2)}{\boldsymbol{P}_{\mathrm{t}}^{-1}(1,2)}\exp\left[-\mathrm{j}(2\psi_1+\psi_2)\right]. \tag{12}$$

where $\psi_1=L_1(\beta_C-\mathrm{j}\alpha_C)$ and $\psi_2=(L_2+L_3)(\beta_C-\mathrm{j}\alpha_C)$.

The output power from the two ports in dB form will be

$$P_{\mathrm{D}}=20\lg\left|\frac{b_8^{'}}{a_0^{'}}\right|, \tag{13}$$

$$P_{\mathrm{B}}=20\lg\left|\frac{b_0^{'}}{a_0^{'}}\right|. \tag{14}$$

The switching characteristics are described below.

(1) Under U=0 V, the switch is operated at drop state, the drop port is named as ON-port, and the through port is named as OFF-port. The insertion loss and crosstalk under this state are characterized as

$$IL_{\mathrm{drop}}=P_{\mathrm{D}}\big|_{U=0}, \tag{15}$$

$$CT_{\mathrm{drop}}=(P_{\mathrm{B}}-P_{\mathrm{D}})\big|_{U=0}. \tag{16}$$

(2) Under the switching voltage, i.e., $U=U_{\mathrm{s}}$, the switch is operated at through state, the vertical output port is named as OFF-port, and the horizontal output port is named as ON-port. The insertion loss and crosstalk under this state are defined as

$$IL_{\mathrm{thr}}=P_{\mathrm{B}}\big|_{U=U_{\mathrm{s}}}, \tag{17}$$

$$CT_{\mathrm{thr}}=(P_{\mathrm{D}}-P_{\mathrm{B}})\big|_{U=U_{\mathrm{s}}}. \tag{18}$$

The resonance order of microring is a key parameter that affects the performance of the MRR EO switch, which should be firstly optimized for obtaining low crosstalk. By using Eqs.(13) and (14), Fig.2(a) shows the output power P_{B} and P_{D} versus operation wavelength λ under different resonance orders, where h_{RR}=0.68 μm, h_{CR}=0.14 μm and U=0 V. It can be found from Fig.2(a) that under different resonance orders, the crosstalks of P_{B}–P_{D} under wavelength of 1550 nm are also different. The curves of crosstalk and insertion loss versus resonance order are further plotted in Fig.2(b). We can find that when m=120, the crosstalk becomes the smallest, and the insertion loss is nearly a constant. So in practical design, we choose m=120, and the corresponding ring radius R is determined to be ~19.49 μm.

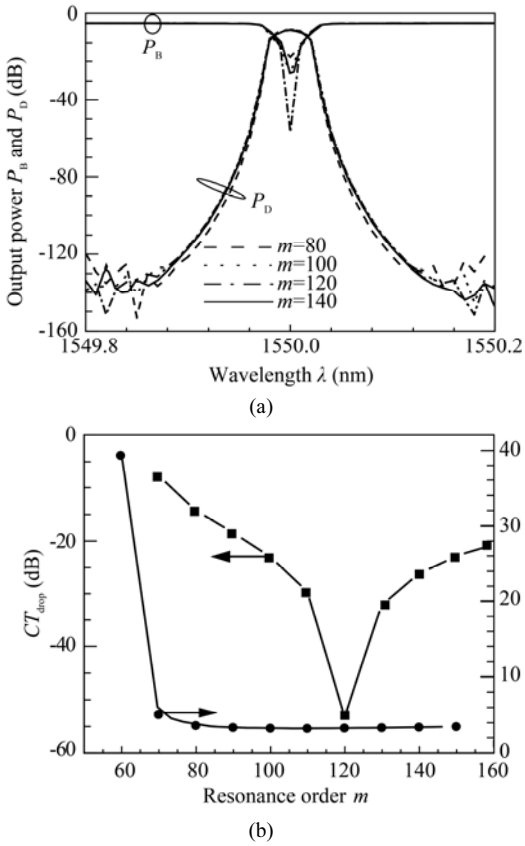

Fig.2 (a) Curves of output power P_{B} and P_{D} versus operation wavelength λ under different resonance orders; (b) Curves of crosstalk and insertion loss under drop state versus resonance order, where h_{RR}=0.68 μm, h_{CR}=0.14 μm and U=0 V

The central coupling gap h_{CR} between channel waveguide and MRR waveguide and the central coupling gap h_{RR} between two adjacent microrings also need to be selected properly. By means of Eqs.(13) and (14), Fig.3(a) shows the output power P_{B} and P_{D} versus operation wavelength λ under different h_{RR}, where h_{CR}=0.14 μm and h_{RR}= 0.38 μm, 0.48 μm, 0.58 μm, 0.68 μm and 0.78 μm. It can be found that h_{RR} affects the output spectral characteristics, such as flat property, insertion loss and crosstalk. When h_{RR}=0.38 μm and 0.48 μm, the spectrum of the drop port is not flat, and the crosstalk is larger than −30 dB. When h_{RR}=0.58 μm or 0.78 μm, though the spectrum of the drop port becomes flat, the crosstalk is still larger than −30 dB. Fig.3(b) shows the curves of the crosstalk and insertion loss versus h_{RR}. When h_{RR}=0.68 μm, the crosstalk becomes the smallest, and under this state, the spectrum is also flat, as seen from Fig.3(a).

Fig.3(c) shows the output power P_{B} and P_{D} versus operation wavelength λ under different h_{CR}, where h_{RR}=0.68 μm, h_{CR}=0.04 μm, 0.14 μm, 0.24 μm and 0.34 μm. It can be found that h_{CR} slightly affects the output spectrum, especially the flat property, but it obviously influences the crosstalk. Fig.3(d) shows the curves of crosstalk and insertion loss versus h_{CR}. When h_{CR}=0.14 μm, the crosstalk becomes the smallest, and the insertion loss nearly be-

comes the smallest. Therefore, we select h_{CR}=0.14 μm and h_{RR}=0.68 μm.

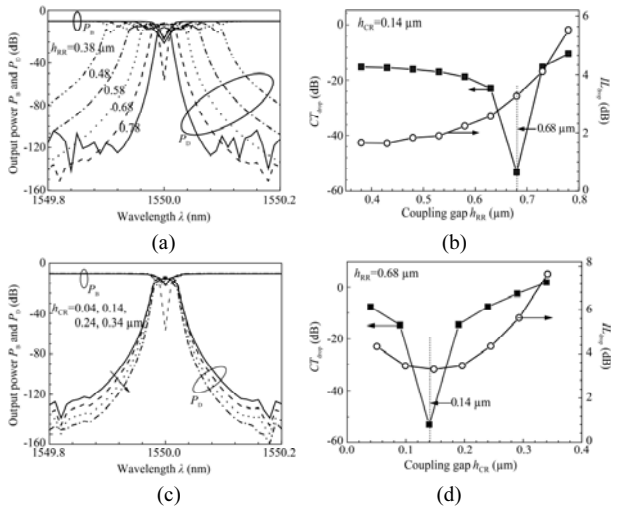

Fig.3 Curves of output power P_B and P_D versus operation wavelength λ under different central coupling gaps: (a) h_{CR}=0.14 μm, λ=1550 nm, h_{RR}=0.38 μm, 0.48 μm, 0.58 μm, 0.68 μm and 0.78 μm, and (c) h_{RR}=0.68 μm, λ=1550 nm, h_{CR} = 0.04 μm, 0.14 μm, 0.24 μm and 0.34 μm; Curves of CT_{dorp} and IL_{dorp} versus (b) h_{RR} and (d) h_{CR}, where λ= 1550 nm

Next, with the optimized parameters above, we investigate the performance of the switch. Fig.4(a) shows the curves of output power P_B and P_D versus the operation voltage U. We can see that when U = 0 V, P_D is the maximum, and the device is operated at drop state. When U increases, P_B increases, P_D decreases, and the through state can be realized. Fig.4(b) shows the result of P_D–P_B versus the applied voltage U, and the relation between P_D–P_B and the device's crosstalk of CT_{drop} and CT_{thr} can be described as

$$P_D-P_B=-CT_{drop},\ P_D-P_B>0, \tag{19}$$

$$P_D-P_B=CT_{thr},\ P_D-P_B<0. \tag{20}$$

When the operation voltage is equal to the switching voltage, the output power from horizontal channel will be the largest, while that output from the vertical channel will be the smallest, thus the switching function is realized. We define the switching voltage for the MRR EO switch as follows for obtaining CT_{thr}=–30 dB, i.e.,

$$U_s=U_s\big|_{CT_{thr}=-30\ \mathrm{dB}}. \tag{21}$$

Then the switching voltage for the device is about 1.86 V.

Fig.5 shows the output spectra of the switch under two operation states (U=0 V for drop state and U=1.86 V for through state). The simulation results indicate that under the applied voltages of 0 V and 1.86 V, the switch presents good switching functions at 1550 nm, and it reveals the boxlike spectral responses for the drop port and the extremely low crosstalk for both states. The crosstalk at through state is −30.2 dB, while that at drop state is about −53.2 dB. The insertion losses at through and drop states are 0.86 dB and 3.18 dB, respectively.

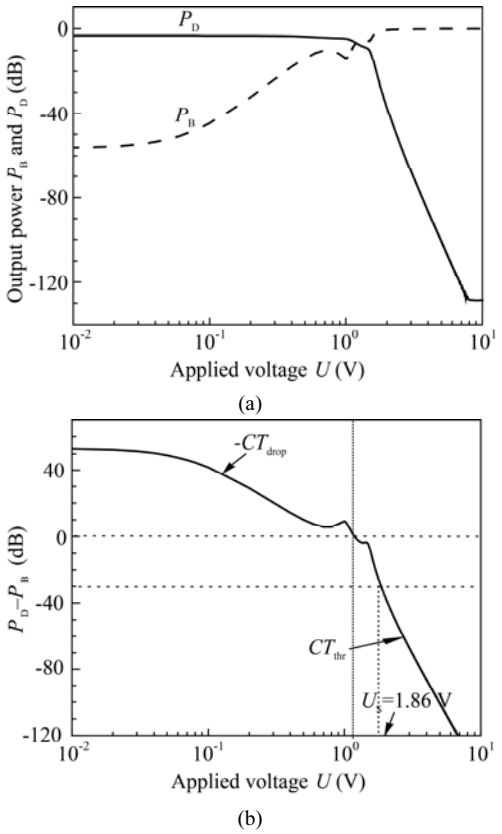

Fig.4 (a) Curves of output power P_B and P_D from the drop and through ports versus the applied voltage U under 1550 nm; (b) Curve of P_D–P_B versus the applied voltage U

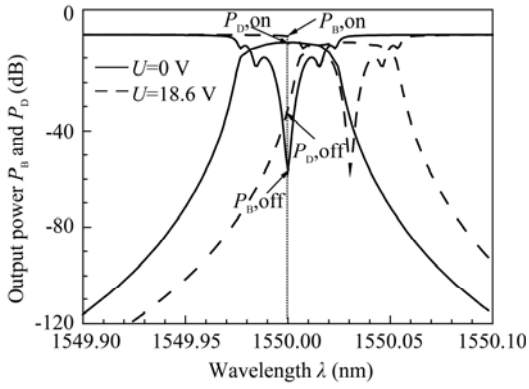

Fig.5 Spectral responses of the MRR switch under drop and through states

In order to confirm the superiority of the MRR switch using seven microrings, we make a comparison on the output spectra of the two switches consisting of seven microrings and one microring, respectively, as shown in Fig.6. The inset of Fig.6 shows the structure of the MRR switch with only one microring cross-coupled with the two channel waveguides. It can be seen that compared with the simple device with only one microring, the

switch with seven vertical-turning serial-coupled microrings reveals favorable flat boxlike spectrum, and the crosstalk is improved greatly from −26.8 dB to −53.2 dB.

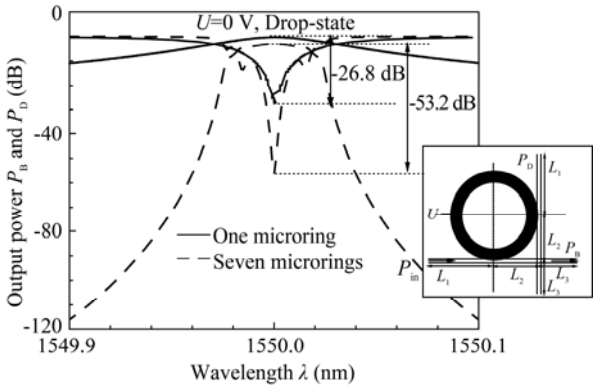

Fig.6 Comparison on the spectral responses of the two MRR switches (drop state) with seven microrings and only one microring, respectively (The inset shows the structure of the MRR switch with only one microring.)

As a conclusion, optimum design and characteristic analysis of a novel MRR EO switch based on seven vertical-tuning serial-coupled microrings are carried out under the operation wavelength of 1550 nm. By selecting proper values of resonance order and central coupling gaps, the crosstalk can be decreased as small as possible, and the output spectrum can be made as flat as possible. Also, compared with the switch with only one microring, the intensity of the non-resonance light can be reduced as weak as possible, and flat boxlike spectrum and low crosstalk can be achieved. Simulation results show that the driving voltage of the device is 1.86 V; the crosstalk at through state is −30.2 dB, while that at drop state is about −53.2 dB; the insertion loss at through state is 0.86 dB, while that at drop state is about 3.18 dB.

References

[1] C. Chen, F. Zhang, H. Wang, X. Sun, F. Wang and D. Zhang, IEEE J. Quantum Electron. **47**, 959 (2011).

[2] A. M. Yan, Y. N. Zhi, J. F. Sun and R. Liu, Appl. Phys. B **107**, 421 (2012).

[3] Y. Enami, D. Mathin, C. T. DeRose, R. A. Norwood, J. Luo, A. K. Y. Jen and N. Peyghambarian, Appl. Phys. Lett. **94**, 213513 (2009).

[4] A. Lorenz and H. S. Kitzerow, Appl. Phys. Lett. **98**, 241106 (2011).

[5] J. Van Campenhout, W. M. Green, S. Assefa and Y. A. Vlasov, Opt. Express **19**, 11568 (2011).

[6] J. Yang, W. Chen, W. Wang, M. Wang and J. Yang, J. Optoelectron. Laser **24**, 16 (2013). (in Chinese)

[7] S. Huang, J. D. Luo, H. L. Yip, A. Ayazi, X. H. Zhou, M. Gould, A. T. Chen, T. Baehr-Jones, M. Hochberg and A. K. Y. Alex, Adv. Mater. **24**, OP1 (2012).

[8] Y. Tsuboi, K. Tsuboi and T. Michinobu, J. Photopolymer Science Technol. **24**, 305 (2011).

[9] C. Cabanetos, E. Blart, Y. Pellegrin, V. Montembault, L. Fontaine, F. Adamietz, V. Rodriguez and F. Odobel, Polymer **52**, 2286 (2011).

[10] X. Yan, C. S. Ma, C. T. Zheng, X. Y. Wang and D. M. Zhang, Opt. Laser Technol. **42**, 526 (2010).

[11] Z. Fan, B. Yun, G. Hu, Y. Yan and Y. Cui, J. Optoelectron. Laser **23**, 1727 (2012). (in Chinese)

[12] G. Y. Xu, Z. F. Liu, J. Ma, B. Y. Liu, S. T. Ho, L. Wang, P. W. Zhu, T. J. Marks, J. D. Luo and A. K. Y. Jen, Opt. Exp. **13**, 7380 (2005).

[13] C. Pitois, S. Vukmirovic, A. Hult, D. Wiesmann and M. Robertsson, Macromolecules **32**, 2903 (1999).

[14] W. G. Driscoll and W. Vaughan, Handbook of Optics, New York: McGraw-Hill, 7 (1978).